Reports of the Department of Mathematical Information Technology
Series B. Scientific Computing
No. B 1/2015

An analytical–numerical study of dynamic stability of an axially moving elastic web

Nikolay Banichuk Alexander Barsuk
Pekka Neittaanmäki Juha Jeronen
Tero Tuovinen

University of Jyväskylä
Department of Mathematical Information Technology
P.O. Box 35 (Agora)
FI–40014 University of Jyväskylä
FINLAND
fax +358 14 260 2771
http://www.mit.jyu.fi/

ISBN 978-951-39-6070-4

978-951-39-6079-7 (PDF)

ISSN 1456-436X

An analytical–numerical study of dynamic stability of an axially moving elastic web*

Nikolay Banichuk Alexander Barsuk Pekka Neittaanmäki
Juha Jeronen Tero Tuovinen

Abstract

This paper is devoted to a dynamic stability analysis of an axially moving elastic web, modelled as a panel (a plate undergoing cylindrical deformation). The results are directly applicable also to the travelling beam. In accordance with the dynamic approach of stability analysis, the problem of harmonic vibrations is investigated via the study of the dependences of the system's natural frequencies on the problem parameters. Analytical implicit expressions for the solution curves, with respect to problem parameters, are derived for ranges of the parameter space where the natural frequencies are real-valued, corresponding to stable vibrations. Both axially tensioned and non-tensioned travelling panels are considered. The special cases of the non-tensioned travelling panel, and the tensioned stationary (non-travelling) panel are also discussed, and special-case solutions given. Numerical evaluation of the obtained general analytical results is discussed. Numerical examples are given for panels subjected to two different tension levels, and for the non-tensioned panel. The results allow the development of very efficient, lightweight solvers for determining the natural frequencies of travelling panels and beams. The results can also be used to help locate the bifurcation points of the solution curves, corresponding to points where mechanical stability is lost.

1 Introduction

The study of the dynamic behaviour of axially moving elastic systems has attracted the attention of researchers for a long time, beginning with Skutch [1897]. Studies written in the English language began to appear half a century later, starting with those by Sack [1954], Archibald and Emslie [1958], Miranker [1960]. Other classic studies of moving elastic systems include those by Mote [1968a,b], Thurman and Mote [1969], Mote [1972], Simpson [1973], Mote [1975], Mujumdar and Douglas

*This research was supported by RFBR (grant 14-08-00016-a), RAS Program 12, Program of Support of Leading Scientific Schools (grant 2954.2014.1), and the Finnish Cultural Foundation.

[1976], Pramila [1986, 1987], Wickert and Mote [1989]. Recent studies include Parker [1998, 1999], Kong and Parker [2004], Wang et al. [2005] and Banichuk et al. [2014b].

Of particular interest for this class of problems is the analysis of stability. A common method of investigating the stability of elastic systems is the dynamic method due to Bolotin [1963]. In accordance with this method, we solve the problem of harmonic vibrations of the investigated system, followed by analysis of the dependence of the behaviour of the natural frequencies as a function of the system parameters.

In the dynamic method, the appearance of complex-valued frequencies is interpreted as a loss of stability in a dynamic form (also known as flutter), corresponding to the loss of Lyapunov stability. A convergence of the frequencies to zero corresponds to a loss of stability in a static form (divergence), and meets the criteria of Euler buckling.

In this paper, we will derive analytical implicit expressions for the solution curves, with respect to problem parameters, for ranges of the parameter space where the natural frequencies are real-valued, corresponding to stable vibrations. Both axially tensioned and non-tensioned travelling panels will be considered. The special cases of the non-tensioned travelling panel, and the tensioned stationary (non-travelling) panel will also be discussed, and special-case solutions given.

In the following sections, we will first set up the problem, after which we will discuss the solution strategy. Then the analytical part of the problem will be solved, and special cases and numerical considerations discussed. Finally, numerical examples will be given.

The results allow the development of very efficient, lightweight solvers for determining the natural frequencies of travelling panels and beams. However, more importantly from a fundamental research perspective, when combined with bifurcation theory, the obtained analytical formulas can also be used to help locate the bifurcation points of the solution curves in the travelling panel (beam) model, corresponding to points where mechanical stability is lost. By a variational argument, it is easily shown that at bifurcation points, the tangent of the local branch of the solution curve in the (V_0, ω) plane becomes vertical (Banichuk et al., 2014a). The obtained analytical formulas can be used as tools to help find such points.

2 Basic relations

Consider an axially travelling rectangular plate undergoing cylindrical deformation, as shown in Figure 1. The equation of small transverse vibrations is

$$m\frac{\partial^2 w}{\partial t^2} + 2mV_0\frac{\partial^2 w}{\partial x \partial t} + (mV_0^2 - T_0)\frac{\partial^2 w}{\partial x^2} + D\frac{\partial^4 w}{\partial x^4} = 0\ , \quad 0 < x < \ell\ , \tag{1}$$

where $m = \rho S$ is the mass of the panel per unit area, ρ is the density of the material, S the area of the cross section, and V_0 is a constant axial transport velocity. The axial tension T_0 has the dimension of force per unit length; for a panel, it can be expressed as $T_0 = h\sigma_x$, where h is the thickness of the panel and σ_x is the axial stress.

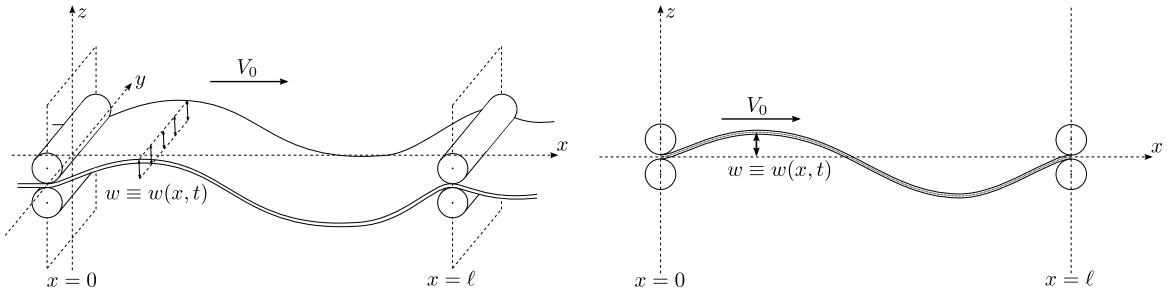

Figure 1: Axially travelling panel, i.e. plate undergoing cylindrical deformation. The pairs of rollers denote simple supports, and the finite thickness depicts the presence of bending resistance. *(a)*: Problem setup. *(b)*: Projection to the xz plane.

The quantity D is the bending rigidity (also known as flexural rigidity or cylindrical rigidity), and for an isotropic elastic material it follows the relation (Timoshenko and Woinowsky-Krieger, 1959)

$$D = \frac{Eh^3}{12(1-\nu^2)} \,, \tag{2}$$

where E is the Young's modulus of the material and ν its Poisson ratio. The symbol ℓ denotes the length of the free span between mechanical supports. The transverse (out-of-plane) displacement of the panel, as it appears in laboratory coordinates (also known as an Eulerian or spatial formulation) is described by the function $w \equiv w(x,t)$.

Equation (1) is of the fourth order in x, so four boundary conditions are needed in total. In what follows, the simply supported (also known as pinned or hinged) boundary conditions of the Kirchhoff plate (or Euler–Bernoulli beam) are used, i.e.

$$w(0,t) = w(\ell,t) = 0 \,, \tag{3}$$

$$D\frac{\partial^2 w}{\partial x^2}(0,t) = D\frac{\partial^2 w}{\partial x^2}(\ell,t) = 0 \,. \tag{4}$$

The boundary conditions (3)–(4) arise by requiring that the transverse displacements and the bending moments at the boundary points $x = 0$ and $x = \ell$ are zero.

Harmonic vibrations of the moving panel are represented as

$$w(x,t) = e^{i\omega t}u(x) \,, \tag{5}$$

where $u(x)$ is the amplitude function and ω is the frequency of vibration. It will be convenient to work in dimensionless variables. Let us define

$$\begin{aligned} x = \ell\tilde{x} \,, \quad \frac{\rho S\omega^2\ell^4}{D} = \tilde{\omega}^2 \,, \quad \frac{\rho S\ell^2}{D}V_0^2 = \tilde{V}_0^2 \,, \\ \frac{\rho S\ell^2}{D}C^2 = \tilde{C}^2 \,, \quad C = \sqrt{\frac{T}{\rho S}} \,. \end{aligned} \tag{6}$$

Note that from the chain rule, $\partial(\cdot)/\partial x \to (1/\ell)\partial(\cdot)/\partial\tilde{x}$. In the following, the tilde will be omitted.

We formulate the boundary-value problem for the amplitude function $u(x)$ as

$$\frac{\mathrm{d}^4 u}{\mathrm{d}x^4} + (V_0^2 - C^2)\frac{\mathrm{d}^2 u}{\mathrm{d}x^2} + 2i\omega V_0 \frac{\mathrm{d}u}{\mathrm{d}x} - \omega^2 u = 0 \ , \quad 0 < x < 1 \ , \tag{7}$$

$$u(0) = u(1) = 0 \ , \quad \left(\frac{\mathrm{d}^2 u}{\mathrm{d}x^2}\right)_{x=0} = \left(\frac{\mathrm{d}^2 u}{\mathrm{d}x^2}\right)_{x=1} = 0 \ . \tag{8}$$

3 Solution strategy

The amplitude function is found as a fundamental solution,

$$u(x) = e^{i\gamma x} \ , \quad 0 < x < 1 \ , \tag{9}$$

of the ordinary differential equation (7) with boundary conditions (8). Here γ is the wave number. Consequently, the displacement function will be described by the expression

$$w = w(x,t) = e^{i\omega t} u(x) = e^{i(\omega t + \gamma x)} \ , \quad 0 < x < 1 \ . \tag{10}$$

Substituting expression (9) into (7), we obtain the characteristic equation

$$\varphi \equiv \gamma^4 - (V_0^2 - C^2)\gamma^2 - 2\omega V_0 \gamma - \omega^2 = 0 \ , \tag{11}$$

where we have defined the polynomial $\varphi \equiv \varphi(\gamma)$.

Let γ_1, γ_2, γ_3 and γ_4 be the roots of the characteristic equation (11). Then we can represent the solution of equation (7) as

$$u(x) = \sum_{k=1}^{4} A_k \exp(i\gamma_k (x - \frac{1}{2})) \ , \tag{12}$$

where A_k ($k = 1, 2, 3, 4$) are arbitrary constants, which can be determined with the help of the boundary conditions (8).

Observe that strictly speaking, the solution (12) only works without modification if all the roots of the polynomial (11) are distinct. As is known from the theory of ordinary differential equations, for example in the case of double roots, the solution will have terms $e^{i\gamma_k x}$ and $xe^{i\gamma_k x}$, where γ_k is the double root. However, in practice, for the present class of systems describing one-dimensional axially travelling elastic materials, this is not a problem, because the roots will almost always be distinct.

In terms of the roots γ_1, γ_2, γ_3 and γ_4, we can write the characteristic equation (11) in the following form (by the fundamental theorem of algebra):

$$\begin{aligned} \varphi &= (\gamma - \gamma_1)(\gamma - \gamma_2)(\gamma - \gamma_3)(\gamma - \gamma_4) \\ &= \gamma^4 - (\gamma_1 + \gamma_2 + \gamma_3 + \gamma_4)\gamma^3 + \left[\gamma_1\gamma_2 + \gamma_3\gamma_4 + (\gamma_1 + \gamma_2)(\gamma_3 + \gamma_4)\right]\gamma^2 \\ &\quad - \left[(\gamma_1 + \gamma_2)\gamma_3\gamma_4 + (\gamma_3 + \gamma_4)\gamma_1\gamma_2\right]\gamma + \gamma_1\gamma_2\gamma_3\gamma_4 = 0 \ . \end{aligned} \tag{13}$$

If we compare the expressions (11) and (13) for φ, and equate the coefficients for like powers of γ, we obtain a system of four algebraic equations

$$\gamma_1 + \gamma_2 + \gamma_3 + \gamma_4 = 0 \ , \tag{14}$$

$$\gamma_1\gamma_2 + \gamma_3\gamma_4 + (\gamma_1 + \gamma_2)(\gamma_3 + \gamma_4) = -(V_0^2 - C^2) \ , \tag{15}$$

$$(\gamma_1 + \gamma_2)\gamma_3\gamma_4 + (\gamma_3 + \gamma_4)\gamma_1\gamma_2 = 2\omega V_0 \ , \tag{16}$$

$$\gamma_1\gamma_2\gamma_3\gamma_4 = -\omega^2 \ . \tag{17}$$

Let us now concentrate on the case where ω is real-valued. It is a general property of the characteristic equation (11), which in this case has real-valued coefficients, that if there exists a complex root of the equation (11), then there exists also a complex conjugate root. In accordance with this observation, it is convenient to introduce new variables s_1, σ_1, s_2 and σ_2 using the relations

$$s_1 = \gamma_1 + \gamma_2 \ , \quad \sigma_1 = \gamma_1\gamma_2 \ , \quad s_2 = \gamma_3 + \gamma_4 \ , \quad \sigma_2 = \gamma_3\gamma_4 \ , \tag{18}$$

and then choose γ_2 and γ_4 to be the complex conjugate values with respect to γ_1 and γ_3, respectively, i.e. $\gamma_2 = \gamma_1^*$ and $\gamma_4 = \gamma_3^*$. Then it follows that the new variables s_1, σ_1, s_2 and σ_2 are always real.

Such a choice is always possible, because the left-hand side of (15) contains all two-element products from the set $\{\gamma_1, \gamma_2, \gamma_3, \gamma_4\}$, and the left-hand side of (16) contains all three-element products. Hence, the particular arrangement of factors used in (15) and (16) is arbitrary. Choosing which of the γ_k represents which root of the characteristic equation is equivalent with first taking some fixed ordering of the roots as given, then rewriting the factorizations in the manner appropriate for that ordering, and finally renumbering the γ_k (and possibly reordering terms) so that the particular form (14)–(17) is obtained.

The roots γ_1, γ_2, γ_3 and γ_4 are expressed in terms of the new variables as

$$\gamma_{1,2} = \frac{1}{2}(s_1 \pm a_1) \ , \quad a_1 = \sqrt{s_1^2 - 4\sigma_1} \ , \tag{19}$$

$$\gamma_{3,4} = \frac{1}{2}(s_2 \pm a_2) \ , \quad a_2 = \sqrt{s_2^2 - 4\sigma_2} \ . \tag{20}$$

Note that (19)–(20) give us a condition for the roots to be distinct: it must hold that $a_1 \neq 0$ and $a_2 \neq 0$.

Using the new variables, equation (13) transforms into the form

$$\varphi = \gamma^4 - (s_1 + s_2)\gamma^3 + (\sigma_1 + \sigma_2 + s_1 s_2)\gamma^2 - (\sigma_1 s_2 + \sigma_2 s_1)\gamma + \sigma_1\sigma_2 = 0 \ . \tag{21}$$

From (14) and (18) it follows that $s_1 + s_2 = 0$, and consequently we may eliminate one variable by defining

$$s \equiv s_1 = -s_2 \ . \tag{22}$$

The relations (14)–(17) are transformed into

$$\sigma_1 + \sigma_2 - s^2 = -(V_0^2 - C^2) \ , \tag{23}$$

$$(\sigma_2 - \sigma_1)s = 2\omega V_0 \ , \tag{24}$$

$$\sigma_1\sigma_2 = -\omega^2 \ . \tag{25}$$

Note that equations (23)–(25) are always valid, regardless of whether the roots of the characteristic equation are distinct, because they follow directly from the characteristic equation.

The solution (12) for the amplitude function $u(x)$ contains arbitrary constants A_k ($k = 1, 2, 3, 4$), which are determined with the help of the boundary conditions (8). Using (12) and (8), we obtain the following system of linear algebraic equations written in matrix form:

$$\mathbf{R}A = 0 \,, \tag{26}$$

where

$$\mathbf{R} = \begin{bmatrix} \psi_1^- & \psi_2^- & \psi_3^- & \psi_4^- \\ -\gamma_1\psi_1^- & -\gamma_2\psi_2^- & -\gamma_3\psi_3^- & -\gamma_4\psi_4^- \\ \psi_1^+ & \psi_2^+ & \psi_3^+ & \psi_4^+ \\ -\gamma_1\psi_1^+ & -\gamma_2\psi_2^+ & -\gamma_3\psi_3^+ & -\gamma_4\psi_4^+ \end{bmatrix} \,, \quad A = \begin{bmatrix} A_1 \\ A_2 \\ A_3 \\ A_4 \end{bmatrix} \,, \tag{27}$$

and

$$\psi_k^+ = \exp(i\frac{\gamma_k}{2}) \,, \quad \psi_k^- = \exp(-i\frac{\gamma_k}{2}) \,, \quad k = 1, 2, 3, 4 \,. \tag{28}$$

The terms involving ψ_k^- follow from boundary conditions at $x = 0$, while the ψ_k^+ terms come from boundary conditions at $x = 1$.

As is well known, a nontrivial solution $A \not\equiv 0$ of the homogeneous linear equation system (26) exists if and only if the determinant is equal to zero, i.e.

$$\Delta = \det \mathbf{R} = 0 \,. \tag{29}$$

Using (19)–(20) and (26)–(28), and performing the necessary transformations, it follows that the solvability condition (29) for the spectral problem (7)–(8) can be represented as

$$\Delta(\omega, V_0) = a_1 a_2 s^2 \left(\cos s - \cos\frac{a_1}{2}\cos\frac{a_2}{2}\right) + \left(s^4 - 2(\sigma_1+\sigma_2)s^2 - 2(\sigma_1-\sigma_2)^2\right)\sin\frac{a_1}{2}\sin\frac{a_2}{2} = 0 \,, \tag{30}$$

$$a_{1,2} = \sqrt{s^2 - 4\sigma_{1,2}} \,.$$

The quantities σ_1 and σ_2, and $s \equiv s_1$ are given by (18). The dependence of Δ on the frequency ω is implicit, via $s = s(\omega, V_0)$, $\sigma_1 = \sigma_1(\omega, V_0)$ and $\sigma_2 = \sigma_2(\omega, V_0)$.

One must be aware that equation (30) depends on the particular form of the solution (12), and thus requires that the roots of the characteristic equation are distinct. If, for some points (ω, V_0), it occurs that (one or both of) $a_1 = 0$ or $a_2 = 0$, then at those points equation (30) cannot be used.

Equation (30) represents a constraint for triples (σ_1, σ_2, s) that give rise to nontrivial solutions of (26). It implicitly eliminates one of σ_1, σ_2 or s. Considered together with the equation system (23)–(25), the remaining unknowns are, in principle, ω and any two of σ_1, σ_2 and s. The axial velocity V_0 is considered a prescribed problem parameter. To obtain the frequency spectrum as a function of V_0, the velocity can be varied quasistatically in the standard manner. Thus, considering the task of determining the wave number parameters γ_k ($k = 1, 2, 3, 4$) and the corresponding free

vibration frequency ω, we have three equations remaining, with three remaining unknowns. The consideration of the boundary conditions, in the form of (26)–(28), has closed the algebraic system, as is indeed expected.

Observe also that due to the periodic nature of (28) with respect to the real part of γ_k, the frequency ω is not unique; there will be a countably infinite spectrum of frequencies ω_j ($j = 1, 2, 3, \dots$), each with its own set of wave numbers γ_k. This is also as expected for the considered class of systems.

Consider next assembling the amplitude function $u(x)$ using (12), after a frequency ω and its corresponding σ_1, σ_2 and s (and hence all four γ_k) are known. When the solvability condition (30) is fulfilled, the matrix $\mathbf{R}$ is singular. Thus, in order to actually determine the values of the A_k from (26), we must eliminate some of the A_k algebraically, until the remaining matrix has full rank (and hence the linear equation system yields a unique solution). To do this, we declare e.g. A_1 a free constant (which is in principle known because any arbitrary value can be assigned to it), and move all terms involving it to the right-hand side.

Typically, one of the A_k will be eliminated, and the solution for $u(x)$ will have one free constant as a global multiplier. To obtain a solution using numerical methods, we may assign e.g. $A_1 = 1$ during the solution process (making numerical elimination possible), and perform the final arbitrary normalization later.

4 Solution of the amplitude equation

In what follows we will consider (23)–(25) as a system of nonlinear equations for the real variables σ_1, σ_2, s. Suppose that $\sigma_1(\omega, V_0)$, $\sigma_2(\omega, V_0)$ and $s(\omega, V_0)$ are two-parameter solutions of the considered system, corresponding to a given value of C. If we substitute the corresponding expressions into (30), we will obtain the implicit equation

$$\Delta(\omega, V_0) = 0 \tag{31}$$

for determination of the frequencies ω of the moving panel, as a function of the panel axial velocity V_0. Note that as pointed out above, equation (31) determines a set of solutions $\omega_j(V_0)$. Also, keep in mind that our solution is valid for the range of velocities at which the frequency ω_j is real-valued.

Let us concentrate on the case where $s \neq 0$. From equations (23)–(24), in this case we have

$$\begin{aligned} \sigma_1 &= \frac{1}{2}\left[s^2 - (V_0^2 - C^2)\right] - \omega\frac{V_0}{s} \,. \\ \sigma_2 &= \frac{1}{2}\left[s^2 - (V_0^2 - C^2)\right] + \omega\frac{V_0}{s} \,. \end{aligned} \tag{32}$$

These equations follow directly from the characteristic equation, under only the assumption that ω is real-valued. Thus, they are valid whenever $s \neq 0$ and $\omega \in \mathbb{R}$; the roots of the characteristic equation need not be distinct.

After substituting (32) into (25) and multiplying the equation by $4s^2$, we find the

relation connecting (ω, V_0, s):

$$s^2 \left[s^2 - (V_0^2 - C^2)\right]^2 = 4\omega^2(V_0^2 - s^2) \ . \tag{33}$$

The same comment as for (32) applies.

Because in our solution range, ω is real-valued, from (33) we also find the following constraint for s:

$$0 < s^2 \leq V_0^2 \ . \tag{34}$$

Equality at the lower limit is not possible in our present solution, because (33) was derived from equations (32), which are valid if $s \neq 0$. Equality at the upper limit holds in the special case $C = 0$; then we have $s = V_0$. This allows us to simplify (30) somewhat; this case will be handled later.

Recalling that C is a known problem parameter, and keeping ω free for now, relation (33) allows us to eliminate one of V_0 or s. Eliminating $s = s(\omega, V_0)$ allows us to write the expression $\Delta(\omega, V_0)$, originally given in terms of s as equation (30), in terms of ω and V_0. However, it should be noted that (33) is a cubic polynomial with respect to the variable s^2; hence its explicit solution is unwieldy to write out, and it is much more convenient in practice to employ a numerical root finder.

As a side remark, observe that the other possibility is to eliminate $V_0 = V_0(\omega, s)$. The polynomial is only quadratic in V_0^2, allowing a short explicit solution (valid where $s \neq 0$ and ω real-valued):

$$V_0^2 = s^2 + C^2 + 2\left(\frac{\omega}{s}\right)^2 \pm 2\sqrt{\left(\frac{\omega}{s}\right)^2 \left(C^2 + \left(\frac{\omega}{s}\right)^2\right)} \ . \tag{35}$$

In practice, the solution with the minus sign for the square root term is the physically relevant one. This would allow us, if we wished, to explicitly find the value of (30) at any point in the (s, ω) plane (with the help of (35), (32) and (30), in that order). However, the physical interpretation of solution curves in the (s, ω) plane is more difficult than for solution curves in the (V_0, ω) plane; thus we will prefer to eliminate s.

Let us return to the task of eliminating $s = s(\omega, V_0)$. We introduce a new positive variable

$$\tau = s^2 \ . \tag{36}$$

Using (36), equation (33) becomes a cubic polynomial equation in τ:

$$\tau^3 - 2(V_0^2 - C^2)\tau^2 + \left[(V_0^2 - C^2)^2 + 4\omega^2\right]\tau - 4\omega^2 V_0^2 = 0 \ . \tag{37}$$

This equation is valid whenever $\tau \neq 0$ (i.e. $s \neq 0$) and $\omega \in \mathbb{R}$.

Observe that a positive solution $\tau > 0$ of (37) exists for any nonnegative values of ω^2 and V_0^2. The constant term of the polynomial depends only on the squares ω^2, V_0^2, and its sign is negative. Hence at $\tau = 0$, the left-hand side of (37) will be ≤ 0, with equality only if $\omega = V_0 = 0$. The sign of the cubic term (which dominates for large $|\tau|$), on the other hand, is positive. The polynomial is continuous as a function of τ. Thus, as τ increases, the polynomial on the left-hand side will inevitably eventually

cross zero at least once. Therefore, because $\tau = s^2$, at least one positive solution of (33) always exists in terms of s^2. Thus (37) determines the dependence $s = s(\omega, V_0)$ (we pick the smallest positive solution for s^2).

For any point in the (ω, V_0) plane, we first determine s from (37). (If $C = 0$, and one wishes to use the general solution procedure, it is possible to use the fact about this special case that $s = V_0$, skipping this step.) Then we use (32) to obtain $\sigma_1(\omega, V_0)$ and $\sigma_2(\omega, V_0)$, and finally, determine the value of $\Delta(\omega, V_0)$ via (30). This allows us to look for solutions of (31) in the (ω, V_0) plane.

5 Special cases

Above, we have treated the general case having $s \neq 0$, for any value for V_0, and with C nonzero. The solution given above is also applicable if $C = 0$ (no axial tension or compression), but in this special case it is possible to simplify the formulas, which we will do next.

We observed that if $C = 0$, then in (34) we have equality at the upper limit, i.e. it holds that $s = V_0$. This allows us to provide the following special-case result. Inserting $C = 0$ and $s = V_0$ into (32), we immediately obtain

$$\left.\begin{aligned} \sigma_1 &= -\omega \\ \sigma_2 &= +\omega \end{aligned}\right\} \ , \quad \text{if } C = 0 \ . \tag{38}$$

Equations (32) were derived under the assumption $s \neq 0$, i.e. in this special case, it would seem we must have $V_0 \neq 0$ in order for (38) to be applicable. However, we may alternatively insert $C = 0$ and $s = V_0$ directly into (23)–(25), which are always valid. We obtain

$$\left.\begin{aligned} \sigma_1 + \sigma_2 &= 0 \\ (\sigma_2 - \sigma_1)V_0 &= 2\omega V_0 \\ \sigma_1\sigma_2 &= -\omega^2 \end{aligned}\right\} \ , \quad \text{if } C = 0 \ . \tag{39}$$

If $V_0 \neq 0$ (i.e. $s \neq 0$), we may proceed to derive the relations (32) as before, and obtain (38). If $V_0 = 0$, the second equation of (39) vanishes identically, and it is easily seen that (38) is a solution satisfying the remaining two equations. Thus we may omit the requirement on V_0.

Substituting (38) into (30) produces first

$$\begin{aligned} a_1 &= \sqrt{V_0^2 + 4\omega} \ , \\ a_2 &= \sqrt{V_0^2 - 4\omega} \ , \end{aligned} \tag{40}$$

and then, for $\Delta(\omega, V_0)$ (after multiplication of both sides by $2/a_1a_2$),

$$\Delta(\omega, V_0) = 2V_0^2 \left(\cos V_0 - \cos \tfrac{\sqrt{V_0^2+4\omega}}{2} \cos \tfrac{\sqrt{V_0^2-4\omega}}{2} \right) + \\ \left(V_0^4 - 8\omega^2\right) \frac{\sin \frac{\sqrt{V_0^2+4\omega}}{2}}{\frac{\sqrt{V_0^2+4\omega}}{2}} \frac{\sin \frac{\sqrt{V_0^2-4\omega}}{2}}{\frac{\sqrt{V_0^2-4\omega}}{2}} = 0 \, . \tag{41}$$

Equation (41) explicitly shows how Δ depends on ω and V_0 in the special case $C = 0$. As for its range of applicability, (41) requires $a_1 \neq 0$ and $a_2 \neq 0$ as before; refer to (40). This is because equation (41) follows from (30), which already has this requirement. Especially, looking at the expression of a_2, we expect equation (30) not to be valid on the curve $\omega = \frac{1}{4}V_0^2$; this will be observed in the numerical results below.

Consider now another special case, where $V_0 = 0$, $\omega \neq 0$ and C free, that corresponds to harmonic vibrations of a stationary (as opposed to axially moving) panel, subjected to extension or compression with load C (which may be zero or nonzero).

In this case, the nonlinear algebraic equation system (23)–(25) takes the form

$$\begin{aligned} \sigma_1 + \sigma_2 &= s^2 + C^2 \, , \\ (\sigma_2 - \sigma_1)s &= 0 \, , \\ \sigma_1\sigma_2 &= -\omega^2 \, . \end{aligned} \tag{42}$$

Starting from the second equation of the system (42) and then proceeding to the other two equations, we obtain two distinct possibilities, namely either

$$s = 0 \, , \quad \sigma_1 + \sigma_2 = C^2 \, , \quad \sigma_1\sigma_2 = -\omega^2 \tag{43}$$

or

$$\sigma_1 = \sigma_2 \equiv \sigma \, , \quad \sigma^2 = -\omega^2 \, , \quad s^2 = 2\sigma - C^2 \, . \tag{44}$$

If $C \neq 0$, the second possibility (44) is not applicable, because ω, σ_1, σ_2 and s are real-valued, and hence $\sigma^2 = -\omega^2$ has no solution except $\sigma = \omega = 0$. This, in turn, leads to $s^2 = -C^2$, which has no real-valued solution for $C \neq 0$.

If $C = 0$, then $\sigma = \omega = s = 0$ is a solution of (44). But this leads to $a_1 = a_2 = 0$, in which case equation (30) is not applicable, and for a full analysis, a new solvability condition must be derived. However, this case is not very interesting, since it implies $\gamma_k = 0$ for all $k = 1, 2, 3, 4$; recall (19)–(20) and (22). This case will be omitted for brevity.

Thus we see that in general, we must pick the first possibility (43). The stationary problem, $V_0 = 0$, is seen to lead to the special case $s = 0$, which was not yet solved. Observe that equations (43) are valid regardless of whether $C \neq 0$ or $C = 0$.

From the last two equations of the system (43), for $s = 0$ we have

$$\begin{aligned} \sigma_1 &= \frac{1}{2}\left[C^2 - \sqrt{C^4 + 4\omega^2}\right] < 0 \, , \\ \sigma_2 &= \frac{1}{2}\left[C^2 + \sqrt{C^4 + 4\omega^2}\right] > 0 \, . \end{aligned} \tag{45}$$

Observe that

$$a_{1,2} = \sqrt{s^2 - \sigma_{1,2}} = \sqrt{-\sigma_{1,2}} \neq 0 \ ,$$

and hence the solvability condition (30) is valid also in this case. From (30), we obtain after inserting $s = 0$ that

$$\begin{aligned} \Delta(\omega,\, V_0{=}0) &= -2\left((\sigma_1 - \sigma_2)^2 \sin\frac{a_1}{2} \sin\frac{a_2}{2}\right) = 0 \ , \\ a_{1,2} &= \sqrt{-4\sigma_{1,2}} \ . \end{aligned} \tag{46}$$

This can be simplified as

$$\begin{aligned} a_1 = 2\sqrt{-\sigma_1} \ , \quad a_2 = 2i\sqrt{\sigma_2} \ , \\ \sin\frac{a_1}{2} = \sin\sqrt{-\sigma_1} \ , \quad \sin\frac{a_2}{2} = i\sinh\sqrt{\sigma_2} \ . \end{aligned} \tag{47}$$

Summarizing, equations (45)–(47) give the solution for the special case $V_0 = 0$, $\omega \neq 0$ and C free.

It was seen that from the case $V_0 = 0$, $\omega \neq 0$, it follows that $s = 0$, but this is a one-way implication. One more special case is thus possible, namely $s = 0$, $V_0 \neq 0$ and C free. From equations (23)–(25), we see that this case leads to

$$\begin{aligned} \sigma_1 + \sigma_2 &= -(V_0^2 - C^2) \ , \\ 0 &= 2\omega V_0 \ , \\ \sigma_1\sigma_2 &= -\omega^2 \ . \end{aligned}$$

Because now $V_0 \neq 0$, from the second equation we obtain $\omega = 0$. That is, for $s = 0$, $V_0 \neq 0$, only the zero frequency is possible. We are left with the system

$$\begin{aligned} \sigma_1 + \sigma_2 &= -(V_0^2 - C^2) \ , \\ \sigma_1\sigma_2 &= 0 \ . \end{aligned} \tag{48}$$

The solution of (48) is

$$\begin{aligned} \sigma_1 &= C^2 - V_0^2 \ , \\ \sigma_2 &= 0 \ . \end{aligned} \tag{49}$$

Now

$$a_{1,2} = \sqrt{s^2 - \sigma_{1,2}} = \sqrt{-\sigma_{1,2}} \ ,$$

whence $a_2 = 0$, and we see that equation (30) cannot be used. Two of the roots of the characteristic equation have coalesced; recall equations (19)–(20). A full analysis requires modifying (12) and deriving a new solvability condition. Because in practice almost always $s \neq 0$, this case is omitted for brevity.

6 Numerical solution of the auxiliary polynomial problem

Noting that equation (30) is implicit, it will be necessary to be able to quickly evaluate it at a large set of points in the (ω, V_0) plane in order to numerically find the zeroes of $\Delta(\omega, V_0)$. This, in turn, requires finding the roots of the cubic polynomial (37) at each point where $\Delta(\omega, V_0)$ is being evaluated.

When programming in a high-level language, the approach providing fastest performance, due to readily allowing vectorization of the cubic polynomial solver, is to use an explicit analytical solution algorithm, such as the one documented in Press and Vetterling [1992, p. 179]. In the following, we briefly review this for the sake of completeness, and give some recommendations on how to produce a fast and reliable solver for the cubic polynomial subproblem of the panel problem under consideration.

Consider the general cubic polynomial

$$ax^3 + bx^2 + cx + d = 0 \,, \tag{50}$$

where $a \neq 0$, and $a, b, c, d \in \mathbb{R}$. Let u_k, where $k = 1, 2, 3$, be the cubic roots of unity:

$$u_1 = 1 \,, \quad u_2 = \frac{1}{2}\left(-1 + \sqrt{3i}\right) \,, \quad u_3 = \frac{1}{2}\left(-1 - \sqrt{3i}\right) \,. \tag{51}$$

Define the quantities

$$\Delta_0 = b^2 - 3ac \,, \tag{52}$$

$$\Delta_1 = 2b^3 - 9abc + 27a^2 d \,, \tag{53}$$

and

$$\delta = \Delta_1^2 - 4\Delta_0^3 \,. \tag{54}$$

It is easy to verify that $\delta = -27a^2\hat{\Delta}$, where $\hat{\Delta}$ denotes the discriminant of the cubic polynomial

$$\hat{\Delta} = 18abcd - 4b^3 d - 4ac^3 - 27a^2 d^2 \,, \tag{55}$$

which determines how the roots behave. Let

$$\hat{C} = \left(\frac{1}{2}\left[\Delta_1 + \sqrt{\delta}\right]\right)^{1/3} \,. \tag{56}$$

With the help of these auxiliary quantities, in the general case the roots of the cubic polynomial (50) are given by

$$x_k = -\frac{1}{3a}\left(b + u_k\hat{C} + \frac{\Delta_0}{u_k\hat{C}}\right) \,, \quad k = 1, 2, 3 \,. \tag{57}$$

The solution splits into four different cases depending on whether Δ_0 and $\hat{\Delta}$ (and thus δ) are zero or nonzero:

1. If $\delta \neq 0$, $\Delta_0 \neq 0$: the general case is applicable. It is valid to take any branch of the square and cube roots in (56), as long as the same branches are taken for every k. Choosing different branches only permutes the roots $x_{1,2,3}$.

2. If $\delta \neq 0$, $\Delta_0 = 0$: the general case is applicable. The branch of the square root in (56) must be chosen such that $\hat{C} \neq 0$. Observe that in this case, $\delta = \Delta_1^2$ and hence $\sqrt{\delta} = \pm\Delta_1$.

3. If $\delta = 0$, $\Delta_0 \neq 0$: there is a double root. The general case is applicable, but the roots also have the alternative representation

$$x_1 = x_2 = \frac{9ad - bc}{2\Delta_0} , \quad x_3 = \frac{4abc - 9a^2d - b^3}{a\Delta_0} .$$

4. If $\delta = 0$, $\Delta_0 = 0$: there is a triple root

$$x_k = -\frac{b}{3a} , \quad k = 1, 2, 3 . \tag{58}$$

   Here the general case is not applicable, because $\hat{C} = 0$.

Considering code vectorization, cases 1–3 can be combined into one code path by modifying (56) to

$$\hat{C} = \left(\frac{1}{2} \left[\Delta_1 + \operatorname{sgn}(\Delta_1) \cdot \sqrt{\delta} \right] \right)^{1/3} , \tag{59}$$

where $\operatorname{sgn}(\cdot)$ is the sign function. Thus, we only need a separate code path for case 4.

The choice of code path for each problem instance is performed efficiently using static branch resolution. We first compute $\hat{C}$ in a vectorized manner for all problem instances using (59). We then set a small tolerance ε (e.g. 10^{-8}), and check for which problem instances it holds that

$$\hat{C}\overline{\hat{C}} > \varepsilon . \tag{60}$$

Problem instances satisfying the check (60) take the general-case code path, while those not satisfying it take the code path for the triple-root special case. In the high-level language, for each value of $k = 1, 2, 3$, only one vectorized computation is needed in each code path, evaluating either (57) or (58), respectively.

When using floating point arithmetic, the explicit solution (57) is not as accurate as the companion matrix method, but almost always the accuracy is sufficient. It is nevertheless good to explicitly zero out very small imaginary parts from the returned x_k before detecting which of the solutions is the real-valued one for each problem instance. In our computations, the tolerance for zeroing out imaginary parts was set to 10^{-10}. The detection of the real-valued solution can then be performed in a vectorized manner.

It should be noted that even in double precision, the explicit solution may fail due to floating point error, if the magnitudes of the coefficients in the polynomial are too disparate. In the panel problem, the coefficients indeed have a large dynamic range. For example, if the load parameter $C = 10$, then in the rectangular area of the (ω, V_0) plane with $10^{-2} \leq \omega \leq 160$ and $10^{-2} \leq V_0 \leq 15$, the largest difference in scales of the polynomial coefficients was found to be approximately 10^8, with the highest-degree coefficient always being $a = 1$, and the constant term d obtaining values between 10^{-8} and 10^8 in different parts of the area tested. When the explicit solution fails, the computed roots can be very far off from the true solution, and for this particular problem, even the sign may be wrong. Although we analytically know that there is always a positive root, in the worst case the numerical solution may come up as negative.

It was considered beyond the scope of this study to determine whether the floating point instability of the explicit solution occurs due to rounding errors or cancellation. Regardless of the cause, there is an easy way to work around the issue. Across the whole plotting range, typically only a very small number of the problem instances exhibit this accuracy issue.

Thus, it is possible to check the residual of the computed solutions against a prescribed small tolerance, and re-compute only the affected solutions using a stable, accurate, but slow (not vectorized) solver, such as a companion matrix based solver. For the residual check, it is best to use the squared residual via the complex norm, because in general the residual is complex-valued. We summed the squared residuals for each k in the same problem instance, and set the tolerance for this sum to 10^{-8}.

This hybrid approach results overall in a fast and reliable solver, requiring only a minimal amount of additional programming. In the same example as above, discretizing the rectangular area into $801 \times 801 = 641\,601$ points, only less than $1\,500$ (i.e. less than 0.3% of the total) of the solutions were detected to require more accurate computation. As an illustrative example, on a normal laptop computer the vectorized hybrid solver for the cubic subproblem performed 60x faster than a simple serial solution (using the accurate solver) of the $641\,601$ problems.

7 Numerical considerations

Let us now consider the full panel problem in the general case. The equations to be solved to obtain a numerical solution are (30), (32) (two equations) and (33). In the numerical examples to follow, we will present the behaviour of the first four frequencies ω, as a function of the panel axial velocity V_0, at some fixed values of the tension parameter C.

To find the solutions, there are several approaches. First, one must be aware that in general, (30) is complex-valued. Although each quantity under the square roots in (30) is real-valued, there is no guarantee that these quantities are non-negative. Indeed, complex values appeared already in the special case $s = 0$, in equations (47).

At closer observation of (30), it is seen that at any point (ω, V_0), either $\mathrm{Re}\,\Delta(\omega, V_0) = 0$ or $\mathrm{Im}\,\Delta(\omega, V_0) = 0$. Because the quantities under the square roots are always real-valued, the square roots are always either purely real or purely imaginary. In practice, it was determined numerically that a_1 is always real, and a_2 obtains both real and imaginary values. Looking at each term of (30), the outcome is that $\Delta(\omega, V_0)$ itself is always either purely real or purely imaginary. Along the curve where $a_2 = 0$, spurious solutions will appear, where both the real and imaginary parts are zero. Solutions along this curve are not valid, because along that curve two of the roots of the characteristic equation coincide, and thus (30) is not applicable there.

In order for a point (ω, V_0) to be a solution of (30), both the real and imaginary parts of $\Delta(\omega, V_0)$ must be zero at that point. Thus, it is convenient to shift our attention to the squared complex norm

$$\|\Delta\|^2 = \Delta\overline{\Delta} = (\mathrm{Re}\,\Delta)^2 + (\mathrm{Im}\,\Delta)^2 \ , \tag{61}$$

which is zero at only such points.

However, as actually computing some values of (61) quickly shows, the values of $\|\Delta\|^2$ are often very large. For example, in the case $C = 10$ with the plotting range set as $10^{-2} \leq \omega \leq 160$ and $10^{-2} \leq V_0 \leq 15$ (the same rectangular area as in the above discussion of the cubic solver), this expression obtains values up to 10^{23} (approximately). This range typically increases when the load parameter C is increased.

Thus, for the purposes of visualization of the values of $\|\Delta\|^2$ and numerical root-finding, it is more convenient to look at e.g.

$$g(\omega, V_0) \equiv \log(1 + \|\Delta\|^2) \ , \tag{62}$$

which reduces the output range to $0 \leq g < 52$ in the same example case. This also makes the gradients of the expression steeper near the solutions. Plots of (62) for $C = 0$, $C = 5$ and $C = 10$ are shown in Figures 2–4.

At any point (ω, V_0), it is computationally very light to evaluate the sequence (37), (32), (30), (61), (62), in that order. Assuming that the complex-valued trigonometric operations in (30) can be performed at least partway in hardware, the computationally heaviest part is the numerical solution of the cubic polynomial (37).

Overall, we can make a rough estimate that with performance-optimized code, one evaluation cycle from given values of (ω, V_0) to the value of (62) should not take more than a few hundred floating point operations per problem instance. The qualitative conclusion is that the function (62) is computationally rather cheap; it is possible to use numerical methods that require a large number of evaluations of the function, and still obtain answers reasonably fast.

One solution approach is to find the minima of (62) by numerical optimization. For any norm, $\|\cdot\| \geq 0$ for any value of the argument, and thus some of the minima can be expected to lie at the zeroes. After the minima are found, their values are easy to check against a small prescribed tolerance. Points at which the value is smaller than the tolerance are then declared to be solutions, and any other minima are discarded.

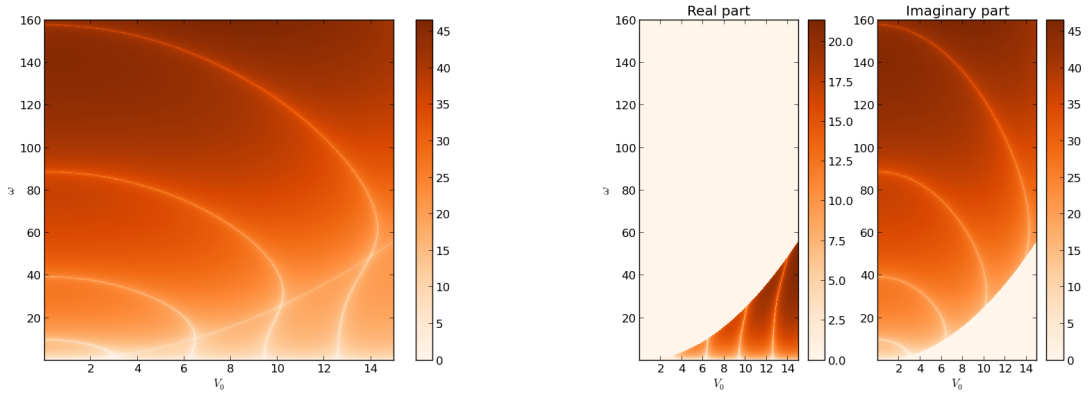

(a) *(b)*

Figure 2: Example with $C = 0$. The natural frequency curves are the zero level sets of the plotted expressions, with the exception of the seam between the real and imaginary regions (refer to subfigure *(b)*), where equation (30) is not valid. With $C = 0$, this seam follows the curve $\omega = \frac{1}{4}V_0^2$; see discussion following equation (41). *(a)*: Expression $g(\omega, V_0) = \log(1 + \|\Delta\|^2)$. *(b)*: Expressions $\log(1 + [\mathrm{Re}\,\Delta]^2)$ and $\log(1 + [\mathrm{Im}\,\Delta]^2)$.

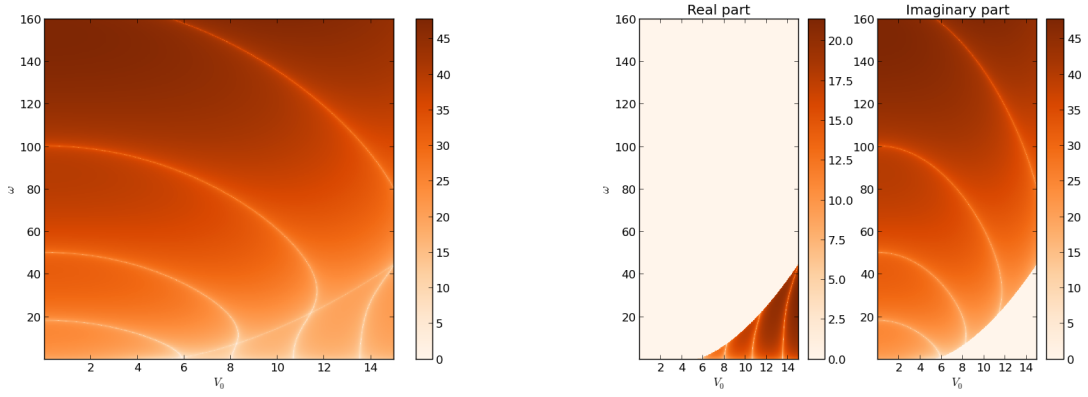

(a) *(b)*

Figure 3: Example with $C = 5$. The natural frequency curves are the zero level sets of the plotted expressions, with the exception of the seam between the real and imaginary regions (refer to subfigure *(b)*), where equation (30) is not valid. *(a)*: Expression $g(\omega, V_0) = \log(1 + \|\Delta\|^2)$. *(b)*: Expressions $\log(1 + [\mathrm{Re}\,\Delta]^2)$ and $\log(1 + [\mathrm{Im}\,\Delta]^2)$.

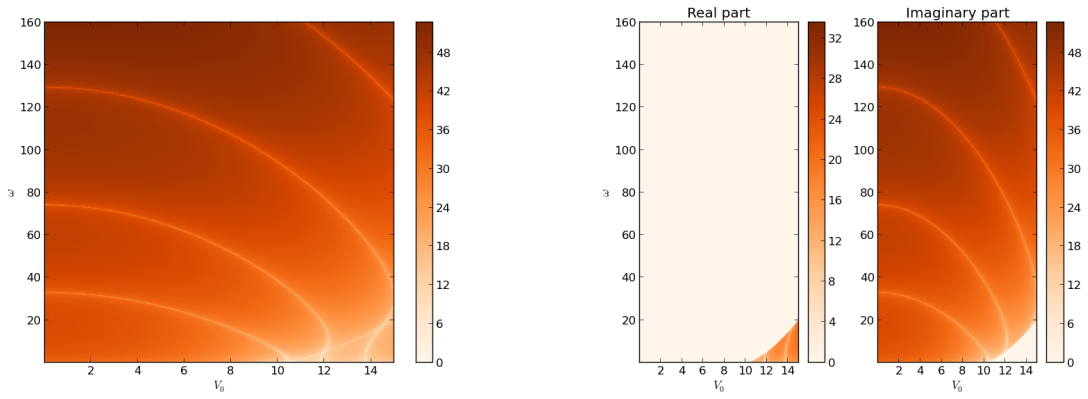

(a) *(b)*

Figure 4: Example with $C = 10$. The natural frequency curves are the zero level sets of the plotted expressions, with the exception of the seam between the real and imaginary regions (refer to subfigure *(b)*), where equation (30) is not valid. *(a)*: Expression $g(\omega, V_0) = \log(1+\|\Delta\|^2)$. *(b)*: Expressions $\log(1+[\mathrm{Re}\,\Delta]^2)$ and $\log(1+[\mathrm{Im}\,\Delta]^2)$.

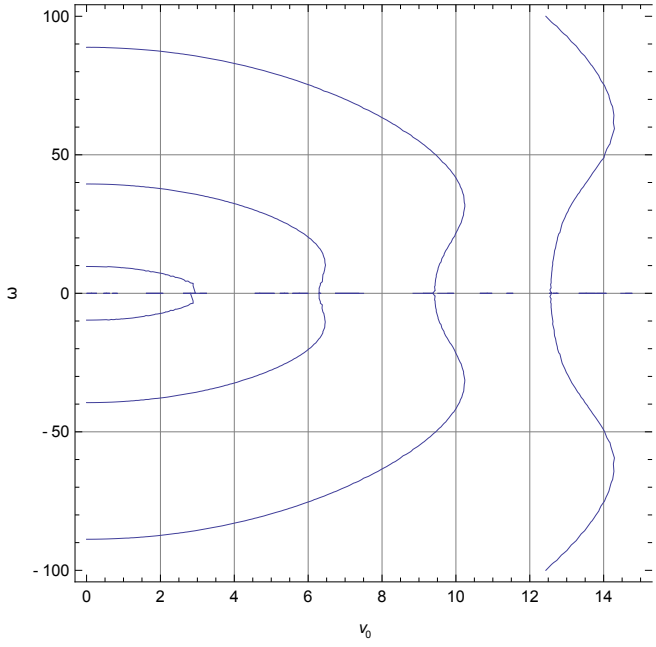

Figure 5: Zero-level set of (30) with $C = 0$, showing the four lowest natural frequencies ω as a function of panel velocity V_0. Produced using the contour plotter of Mathematica, directly searching for the zero level set of the complex-valued expression (41). Note good quality in most part of the plotting area, and accuracy problems near the V_0 axis especially in the lowest mode.

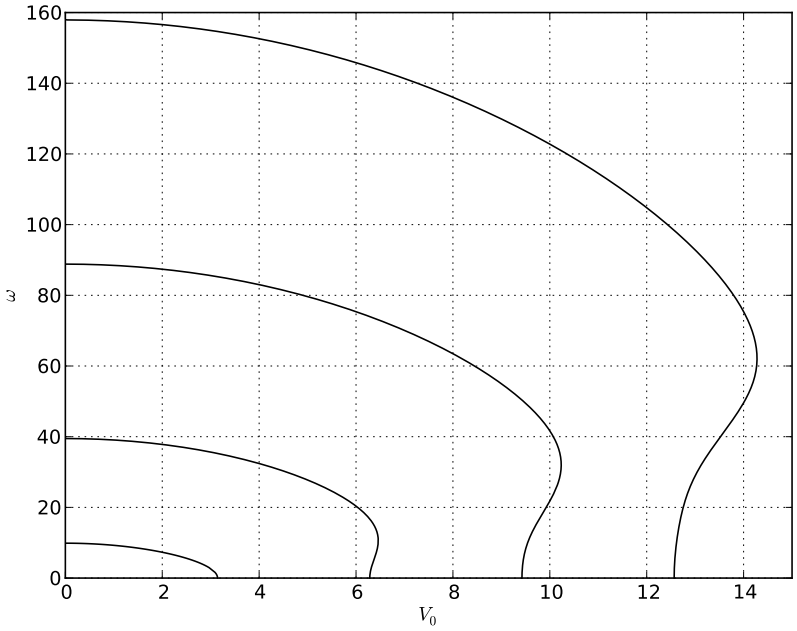

Figure 6: Four lowest natural frequencies ω as a function of panel velocity V_0. Tension load parameter $C = 0$.

The optimization process can be simplified into one input dimension, keeping V_0 fixed, or alternatively, keeping ω fixed. Another variant is to estimate the local tangent of the solution curve, and optimize parametrically in the direction orthogonal to it. The reduction to one dimension makes the optimization problem much easier numerically, and also saves computational resources. However, a simple local optimizer alone is not sufficient for this problem, because several branches of the solution (zeroes of the complex norm) may reside in the plotting range, and all of them must be found.

Another approach to visualize the solution is to draw the zero level set of (30) using a contour plotter, but this requires very high accuracy and thus cannot be generally recommended. See Figure 5 for an example in the case $C = 0$, using the special case formula (41).

The final results for $C = 0$, $C = 5$ and $C = 10$ are shown in Figures 6–8, respectively. To produce these figures, we have first plotted (62) on a cartesian grid of 801×801 points (as shown in Figures 2a–4a), and visually determined the points where the solution curves cross the V_0 and ω axes. Then, using these points as starting values, we have numerically tracked the solutions. For the purposes of tracking, the plot area shown in the figures was scaled to have square aspect ratio, and the tracking step size was set to 0.25% of plot area width.

Each solution point was obtained by local minimization of (62) along a bounded line segment orthogonal to the local tangent of the curve. The bounds for the optimization were chosen as $\pm 5\,\Delta x$, where Δx is the tracking step size. Because the

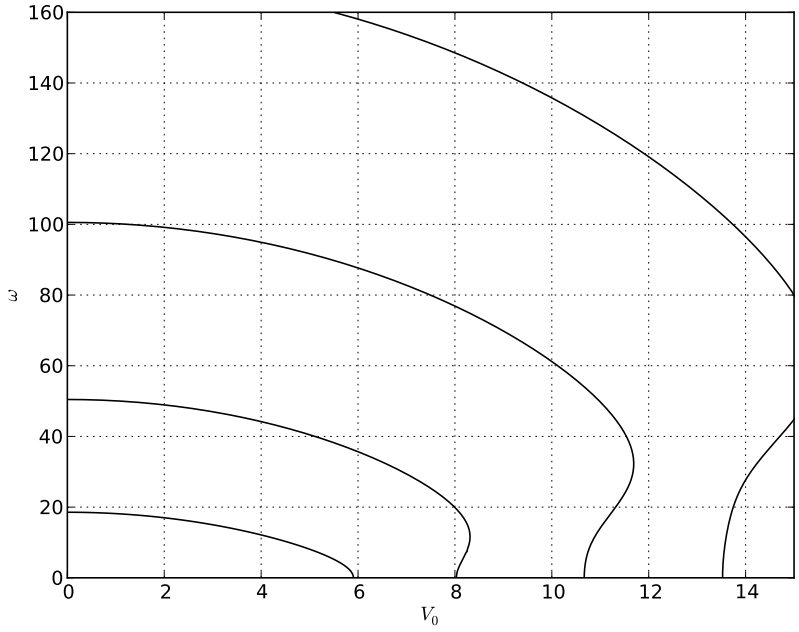

Figure 7: Four lowest natural frequencies ω as a function of panel velocity V_0. Tension load parameter $C = 5$.

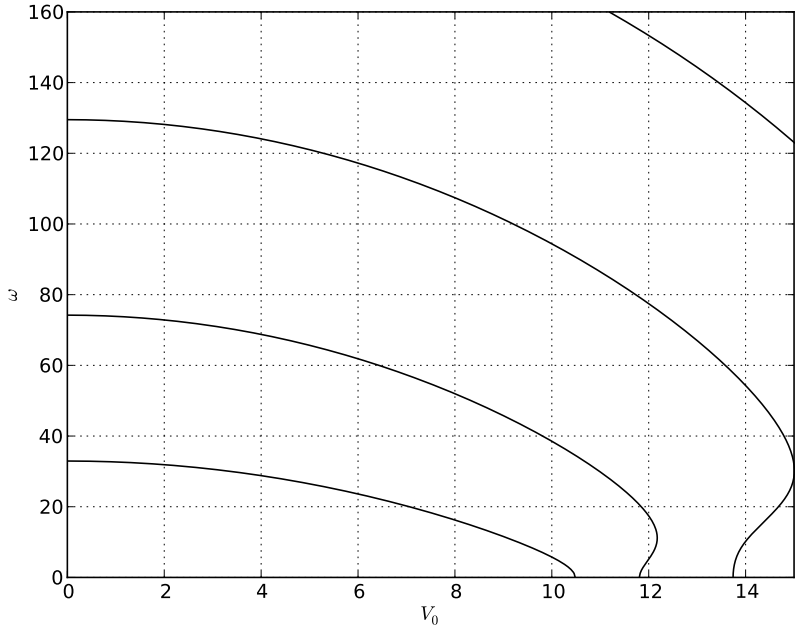

Figure 8: Four lowest natural frequencies ω as a function of panel velocity V_0. Tension load parameter $C = 10$.

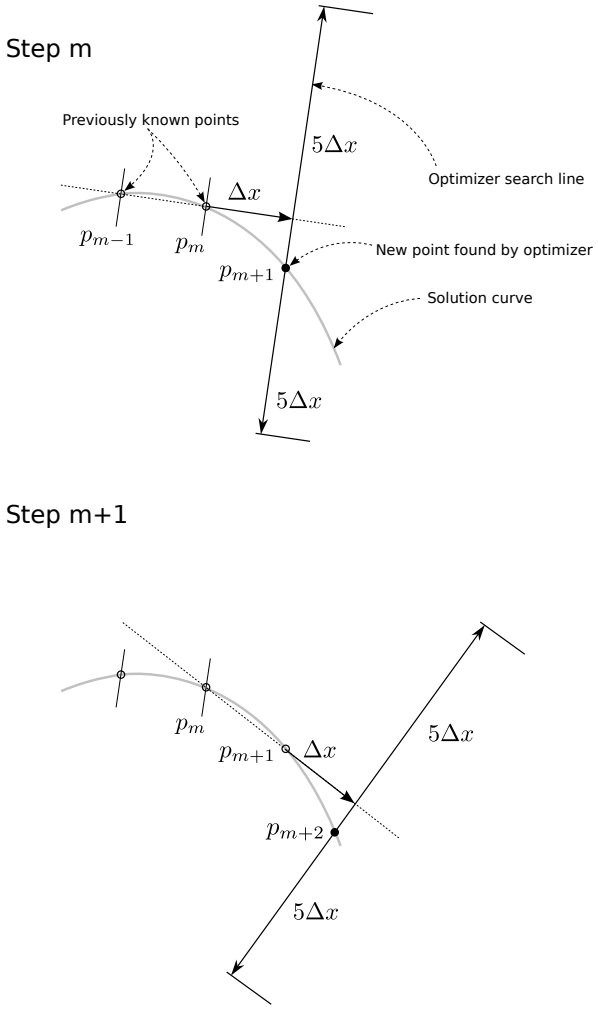

Figure 9: Solution curve tracking strategy.

starting values are well-chosen and the curves are continuous, it is known beforehand that the local minimum found at each step will lie at a zero of (62), and no tolerance check is needed. See Figure 9 for the idea.

The tangent of the curve was initially taken to be orthogonal to the axis, and at all further steps, the tangent direction was approximated as the difference vector between the latest two known solution points. Technically, this gives the first-order backward difference of the tangent at the *last known* solution point, but in practice this was found to be accurate enough for setting the search range for the optimizer. For each solution curve, the tracking proceeds independently from each axis, and stops at the seam where $\Delta(\omega, V_0)$ switches from real to imaginary or vice versa. This produces two independent solution curve segments for each solution curve.

When approaching the seam, the tracking process often catches a point or two on the spurious solution curve. These points were filtered out in a separate post-processing step, utilizing the fact that the solution curves are at least C^1 continu-

ous. In practice, this was implemented as a difference-based local tangent check. Each vector of points (solution curve segment) produced by the tracking phase was checked such that if the angle between the direction vectors determined by two successive point pairs (p_m, p_{m-1}) and (p_{m+1}, p_m) is more than 5 degrees, the points from $m+1$ onward (inclusive) are discarded and the postprocessing for that curve segment ends. After both segments belonging to the same solution curve have been postprocessed, the segments are joined and plotted. The solutions behave smoothly enough near the seam that linear interpolation (which the plotter performs) between the last non-discarded points is accurate enough to produce a smooth-looking visualization (refer to Figures 6–8 for examples).

8 Conclusion

Analytical studies of the dynamic behaviour of moving elastic systems are very important from both theoretical and practical points of view, and have attracted the attention of many researchers working in the domain of theoretical and applied mechanics. Of particular interest has been the problem of elastic stability of a moving band and the application of dynamic analysis.

In the present study, in accordance with the dynamic approach of stability analysis, the problem of harmonic vibrations was investigated via the study of the dependences of the system's natural frequencies on the problem parameters. Analytical implicit expressions for the solution curves, with respect to problem parameters, were derived for ranges of the parameter space where the natural frequencies are real-valued, corresponding to stable vibrations. Both axially tensioned and non-tensioned travelling panels were considered.

The special cases of the non-tensioned travelling panel, and the tensioned stationary (non-travelling) panel are also discussed, and special-case solutions given. Numerical evaluation of the obtained general analytical results was discussed, and numerical examples were given for panels subjected to two different tension levels, and for the non-tensioned panel.

The performed analytical studies show in an explicit form the nature of the mechanical instability for the travelling panel (and beam) model. The results allow the development of very efficient, lightweight solvers for determining the natural frequencies of travelling panels and beams.

However, more importantly from the viewpoint of fundamental studies of axially moving materials, the results can be used to help locate the bifurcation points of the solution curves, corresponding to points where mechanical stability is lost. By a variational argument, it is easily shown that at the bifurcation points, the tangent of the local branch of the solution curve in the (V_0, ω) plane becomes vertical (Banichuk et al., 2014a); the obtained analytical formulas can be used to help find such points.

Acknowledgements

This research was supported by RFBR (grant 14-08-00016-a), RAS Program 12, Program of Support of Leading Scientific Schools (grant 2954.2014.1), and the Finnish Cultural Foundation.

References

F. R. Archibald and A. G. Emslie. The vibration of a string having a uniform motion along its length. *ASME Journal of Applied Mechanics*, 25:347–348, 1958.

N. Banichuk, A. Barsuk, T. Tuovinen, and J. Jeronen. Variational approach for analysis of harmonic vibration and stability of moving panels. *Rakenteiden mekaniikka (Finnish Journal of Structural Mechanics)*, 47(4):148–162, 2014a.

N. Banichuk, J. Jeronen, P. Neittaanmäki, T. Saksa, and T. Tuovinen. *Mechanics of moving materials*, volume 207 of *Solid mechanics and its applications*. Springer, 2014b. ISBN: 978-3-319-01744-0 (print), 978-3-319-01745-7 (electronic).

V. V. Bolotin. *Nonconservative Problems of the Theory of Elastic Stability*. Pergamon Press, New York, 1963.

L. Kong and R. G. Parker. Approximate eigensolutions of axially moving beams with small flexural stiffness. *Journal of Sound and Vibration*, 276:459–469, 2004. URL `http://dx.doi.org/10.1016/j.jsv.2003.11.027`.

W. L. Miranker. The wave equation in a medium in motion. *IBM Journal of Research and Development*, 4:36–42, 1960. URL `http://dx.doi.org/10.1147/rd.41.0036`.

C. D. Mote. Divergence buckling of an edge-loaded axially moving band. *International Journal of Mechanical Sciences*, 10:281–195, 1968a.

C. D. Mote. Dynamic stability of an axially moving band. *Journal of the Franklin Institute*, 285(5):329–346, May 1968b.

C. D. Mote. Dynamic stability of axially moving materials. *Shock and Vibration Digest*, 4(4):2–11, 1972.

C. D. Mote. Stability of systems transporting accelerating axially moving materials. *ASME Journal of Dynamic Systems, Measurement, and Control*, 97:96–98, 1975.

A. S. Mujumdar and W. J. M. Douglas. Analytical modelling of sheet flutter. *Svensk Papperstidning*, 79:187–192, 1976.

R. G. Parker. On the eigenvalues and critical speed stability of gyroscopic continua. *ASME Journal of Applied Mechanics*, 65:134–140, 1998. URL `http://dx.doi.org/10.1115/1.2789016`.

R. G. Parker. Supercritical speed stability of the trivial equilibrium of an axially-moving string on an elastic foundation. *Journal of Sound and Vibration*, 221(2): 205–219, 1999. URL `http://dx.doi.org/10.1006/jsvi.1998.1936`.

A. Pramila. Sheet flutter and the interaction between sheet and air. *TAPPI Journal*, 69(7):70–74, 1986.

A. Pramila. Natural frequencies of a submerged axially moving band. *Journal of Sound and Vibration*, 113(1):198–203, 1987.

W. H. Press and W. T. Vetterling. *Numerical Recipes in Fortran 77: The Art of Scientific Computing*. Cambridge University Press, 1992. ISBN 0-521-43064-X.

R. A. Sack. Transverse oscillations in traveling strings. *British Journal of Applied Physics*, 5:224–226, 1954.

A. Simpson. Transverse modes and frequencies of beams translating between fixed end supports. *Journal of Mechanical Engineering Science*, 15:159–164, 1973. URL http://dx.doi.org/10.1243/JMES_JOUR_1973_015_031_02.

R. Skutch. Uber die Bewegung eines gespannten Fadens, weicher gezwungen ist durch zwei feste Punkte, mit einer constanten Geschwindigkeit zu gehen, und zwischen denselben in Transversal-schwingungen von gerlinger Amplitude versetzt wird. *Annalen der Physik und Chemie*, 61:190–195, 1897.

A. Thurman and C. Mote, Jr. Free, periodic, nonlinear oscillation of an axially moving strip. *Journal of Applied Mechanics*, 36(1):83–91, Mar. 1969. URL http://dx.doi.org/doi:10.1115/1.3564591.

S. P. Timoshenko and S. Woinowsky-Krieger. *Theory of plates and shells*. New York : Tokyo : McGraw-Hill, 2nd edition, 1959. ISBN 0-07-085820-9.

Y. Wang, L. Huang, and X. Liu. Eigenvalue and stability analysis for transverse vibrations of axially moving strings based on Hamiltonian dynamics. *Acta Mechanica Sinica*, 21:485–494, 2005. URL http://dx.doi.org/10.1007/s10409-005-0066-2.

J. A. Wickert and C. D. Mote, Jr. On the energetics of axially moving continua. *The Journal of the Acoustical Society of America*, 85(3):1365–1368, 1989. URL http://link.aip.org/link/?JAS/85/1365/1.